J. Braz. Chem. Soc., Vol. 17, No. 7, 1368-1376, 2006.
Printed in Brazil - ©2006 Sociedade Brasileira de Química
0103 - 5053 $6.00+0.00

Article

Photophysical and Photocatalytic Properties of Novel M_2BiNbO_7 (M = In and Ga)

Jingfei Luan,*[*,a] Shourong Zheng,[a] Xiping Hao,[b] Guoyou Luan,[c] Xiaoshan Wu[b] and Zhigang Zou[d]

[a]*State Key Laboratory of Pollution Control and Resource Reuse, School of Environment, Nanjing University, Nanjing, 210093 People's Republic of China*

[b]*National Laboratory of Solid State Microstructures, Nanjing University, Nanjing 210093, People's Republic of China*

[c]*State Key Laboratory of Catalysis, Dalian Institute of Chemical Physics, Chinese Academy of Sciences, Dalian 116023, People's Republic of China*

[d]*Eco-Materials and Renewable Energy Research Center, Nanjing University, Nanjing 210093, People's Republic of China*

Os óxidos M_2BiNbO_7 (M = In e Ga) foram sintetizados através de reações no estado sólido, e suas propriedades estruturais e fotocatalíticas, investigadas. Os resultados indicaram que estes compostos cristalizam na estrutura do tipo pirocloro, no sistema cúbico, grupo espacial Fd-3m. Os valores estimados dos "band gaps" dos óxidos In_2BiNbO_7 e Ga_2BiNbO_7 são 2,52(5) e 2,57(8) eV, respectivamente. A reação fotocatalítica da decomposição de água pura foi estudada na presença dos fotocatalisadores M_2BiNbO_7 (M = In e Ga) e irradiação no ultravioleta, através do monitoramento da formação de H_2 e de O_2. A degradação fotocatalítica do corante azul de metileno em água, na presença destes óxidos, foi investigada sob irradiação no visível. Os catalisadores M_2BiNbO_7 (M = In e Ga) mostraram-se mais ativos do que o P-25, nessas condições. Completa degradação do azul de metileno foi observada após irradiação no visível durante 160 minutos, na presença do fotocatalisador Ga_2BiNbO_7, e após 180 minutos na presença de In_2BiNbO_7. A diminuição do teor total de carbono (TOC) e a formação dos produtos SO_4^{2-} e NO_3^- confirmaram a mineralização do azul de metileno durante o processo fotocatalítico.

M_2BiNbO_7 (M = In and Ga) were synthesized by solid-state reaction method and their structural and photocatalytic properties were investigated. The results indicated that these compounds crystallize in the pyrochlore-type structure, cubic system with space group Fd-3m. In addition, the band gaps of In_2BiNbO_7 and Ga_2BiNbO_7 were estimated to be about 2.52(5) and 2.57(8) eV, respectively. For the photocatalytic water splitting reaction, H_2 or O_2 evolution was observed from pure water respectively with M_2BiNbO_7 (M = In and Ga) as the photocatalysts under ultraviolet light irradiation. Photocatalytic degradation of aqueous methylene blue (MB) dye over these compounds was further investigated under visible light irradiation. M_2BiNbO_7 (M = In and Ga) showed markedly higher catalytic activity compared to P-25 for MB photocatalytic degradation under visible light irradiation. Complete removal of aqueous MB was observed after visible light irradiation for 160 min with the Ga_2BiNbO_7 as the photocatalyst and for 180 min with the In_2BiNbO_7 as the photocatalyst. The decrease of the total organic carbon (TOC) and the formation of inorganic products, SO_4^{2-} and NO_3^-, demonstrated the continuous mineralization of aqueous MB during the photocatalytic process.

Keywords: inorganic photocatalysts, crystal structure, removal of methylene blue dye, band structure, visible light irradiation

Introduction

Since Honda and Fujishima first observed the splitting of water on TiO_2 electrode in 1972,[1] the investigation of semiconductor photocatalysts has attracted much attention from both academic and industrial societies.[2,3] The photocatalytic water splitting using solar energy to produce hydrogen gas is crucial owing to the emergent requirement of clean and renewable sources.[2-4] Up to now, some photocatalysts with different structures have been

*e-mail: jfluan@nju.edu.cn

synthesized to investigate the effective utilization of solar energy. Among them, some Nb-containing photocatalysts with a pyrochlore-type structure were reported recently, such as Bi_2MNbO_7 ($M = Al^{3+}$, Ga^{3+}, In^{3+})[5] and Bi_2RNbO_7 (R = Y, rare earth elements).[6]

In addition, scientific interest in the photocatalytic degradation of aqueous organic pollutants has quickly increased recently.[7-9] In particular, it was reported that 15% of the total world production of dyes is lost during the dyeing process and is released to the textile effluents, which eventually pollute the groundwater. The release of those colored waste waters in the ecosystem is a dramatic source of non-aesthetic pollution, eutrophication and perturbations in the aquatic life. Many reports have revealed that the organic dyes could be effectively degraded using the TiO_2-based photocatalytic process; however, the degradation of a majority of organic dyes are only under UV irradiation except for some dyes, such as alizarin red, which can be degraded under visible light using the TiO_2-based photocatalysts based on the dye-sensitized process.[10,11] Among different dyes, methylene blue dye (MB) is difficult to be decomposed under visible light irradiation and is usually regarded as a model dye contaminant to evaluate the activity of a photocatalyst.[12,13] Up to now, there were only few reports of MB dye degradation under visible light irradiation.[12,14] Therefore, it is highly desirable to develop new visible light-driven photocatalysts with high activity.

It has been generally observed that numerous compounds with the $A_2B_2O_7$ pyrochlore structure display antiferroelectric phases or dielectric abnormality. However, only a few compounds display ferroelectric behavior.[15,16] M_2BiNbO_7 (M = In and Ga) belongs to the family of the $A_2B_2O_7$ compounds, but the data about its space group and lattice constants have not been reported previously. Moreover, no photocatalytic properties of M_2BiNbO_7 (M = In and Ga) have been investigated so far. We considered that In^{3+} or Ga^{3+} occupying the A site and Bi^{3+} occupying the B site in the $A_2^{3+}B_2^{4+}O_7$ compounds may lead to an increase in hole (carrier) concentration, and thus result in a change in the electrical transportation and photophysical properties. We also speculate that M_2BiNbO_7 (M = In and Ga) might yield a slight modification of crystal structure and result in a change in photophysical properties. It is noteworthy that a slight modification in the structure of a semiconductor will lead to a marked change in photocatalytic properties.[8] In this contribution, we prepared the M_2BiNbO_7 (M = In and Ga) photocatalysts and the structural and photocatalytic properties of M_2BiNbO_7 (M = In and Ga) were studied in detail. A comparison of the photocatalytic property of M_2BiNbO_7 (M = In and Ga) with that of TiO_2 (P-25) is also provided.

Experimental

The polycrystalline samples of the photocatalysts were synthesized by a solid-state reaction method. Ga_2O_3, In_2O_3, Bi_2O_3 and Nb_2O_5 (China Medicine (Group) Shanghai Chemical Reagent Corporation) with purity of 99.99% were used as starting materials. The powders were dried at 200 °C for 4 h. Then the stoichiometric amounts of precursors were mixed and pressed into small columns. At last the small columns were sintered at 1100 °C for 52 h in an alumina crucible (ShenYang Crucible Co., LTD, China) with an electric furnace (KSL 1700X, Hefei Kejing Materials Technology CO., LTD, China). The crystal structure of M_2BiNbO_7 (M = In and Ga) was analyzed by the X-ray diffractometer (D/MAX-RB, Rigaku Corporation, Japan) with Cu*K*α radiation (λ = 1.54056). The data were collected at 295 K with a step scan procedure in the range of 2θ = 5-100°. The step interval was 0.02° and the scan speed was 1° min^{-1}. The chemical composition of the compound was measured by scanning electron microscope-X-ray energy dispersion spectrum (SEM-EDX, (LEO 1530VP, LEO Corporation, Germany)) and X-ray Fluorescence spectrometer (ARL-9800, ARL Corporation, Switzerland). The optical absorption of M_2BiNbO_7 (M = In and Ga) was analyzed with an UV-Visible spectrophotometer (Lambda 35, Perkin-Ebmer Corporation, USA). The surface areas were determined using the BET method (MS-21, Quantachrome Instruments Corporation, USA) with N_2 adsorption at liquid nitrogen temperature.

The photocatalytic degradation of aqueous MB was performed with 0.5 g Ga_2BiNbO_7 or In_2BiNbO_7 or TiO_2 powders suspended in 100 mL methylene blue solution (MB solution concentration was 0.0506 mol m^{-3} and the initial pH value of the solution was 7) in a pyrex glass cell (Jiangsu Yancheng Huaou Industry, China). The photocatalytic reaction system consisted of a 300 W Xe arc lamp (Nanjing JYZCPST CO., LTD) and a cut-off filter (λ > 420 nm, Jiangsu Nantong JSOL Corporation, China). The concentration of MB was determined with a UV-Vis spectrometer (UV-2201, Shimadzu Corporation, Japan) with the detecting wavelength at 670 nm. The inorganic products of MB degradation were detected by ion chromatograph (DX-300, Dionex Corporation, USA). Total organic carbon (TOC) was determined with a TOC analyzer (TOC-5000, Shimadzu Corporation, Japan).

The photocatalytic water splitting with M_2BiNbO_7 (M = In and Ga) as the photocatalysts was carried out in pure water (1.0 g powder catalyst, 300 mL H_2O) under UV irradiation. The catalysts were suspended in pure water by a magnetic stirrer and the photocatalytic reaction was conducted in a gas closed circulation system with an inner-irradiation type quartz cell and a 400 W high-pressure Hg lamp (Beijing Dongsheng Glass Light Source Factory, China).

Results and Discussion

Structural properties

Figure 1 shows X-ray diffraction patterns of M_2BiNbO_7 (M = In and Ga) sintered at 1100 °C in air. The powder X-ray diffraction analysis showed that M_2BiNbO_7 (M = In and Ga) are single phase, which is consistent with the results from SEM-EDX. The chemical composition of M_2BiNbO_7 (M = In and Ga) was measured with the ZAF (element number, absorption and fluorescence corrections) quantification method. The SEM-EDX analysis revealed that M_2BiNbO_7 (M = In and Ga) had a homogenous atomic distribution with no other impure elements. An average atomic rate of Ga: Bi: Nb = 2.00: 0.98: 1.02 for Ga_2BiNbO_7 and In: Bi: Nb = 2.00: 0.97: 1.03 for In_2BiNbO_7 was obtained from measurements at different points. The results are in good agreement with the measurement from X-ray fluorescence spectrometer. Based on the above results, we can conclude that the resulting materials are of high purity under our preparation conditions. The morphology of M_2BiNbO_7 (M = In and Ga) is described in Figure 2. It was shown that the particle distribution was homogeneous and the average particle diameters of In_2BiNbO_7 and Ga_2BiNbO_7 were estimated to be 1.5 and 1.7 μm.

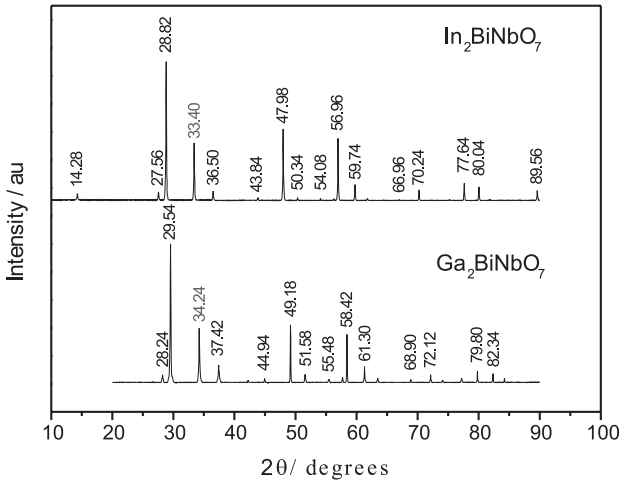

Figure 1. X-ray powder diffraction patterns of the M_2BiNbO_7 (M = In and Ga) photocatalysts at 1100 °C.

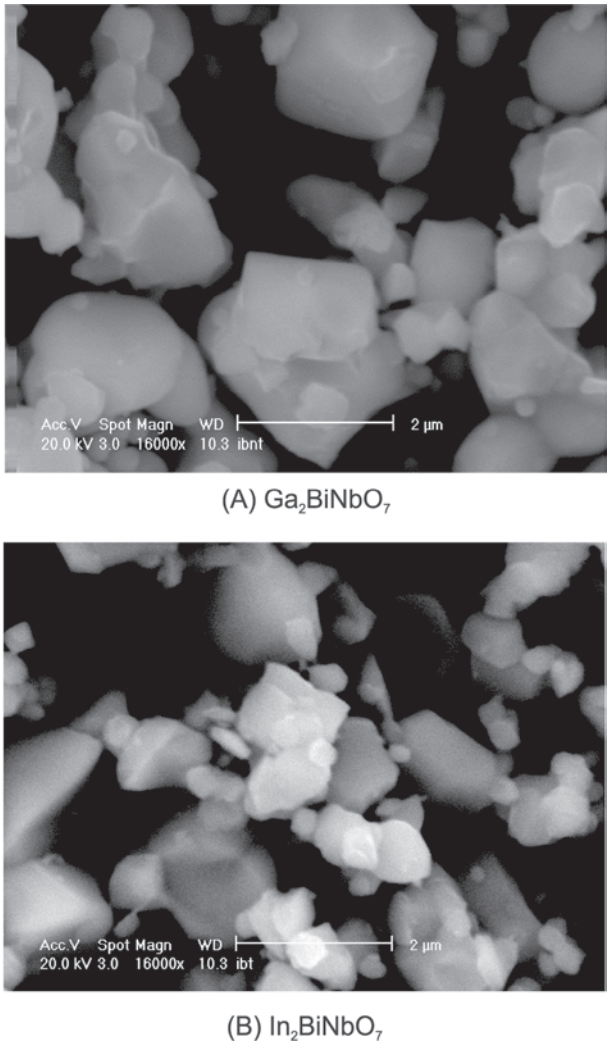

Figure 2. SEM morphology of the M_2BiNbO_7 (M = In and Ga) photocatalysts: (a) Ga_2BiNbO_7 and (b) In_2BiNbO_7.

Full-profile structure refinement of the collected powder diffraction data for M_2BiNbO_7 (M = In and Ga) was conducted using the Rietveld program REITAN,[17] by which positional parameters and isotropic thermal parameters of M_2BiNbO_7 (M = In and Ga) were refined. The atomic coordinates and isotropic thermal parameters of M_2BiNbO_7 (M = In and Ga) are listed in Table 1 and Table 2. The result of the final refinement for M_2BiNbO_7 (M = In and Ga) indicated a good agreement between the observed and calculated intensities in the pyrochlore type crystal structure of the cubic system with space group Fd-3m when the O atoms are included in the model. The lattice parameter is found to be a = 10.4685(5) Å for Ga_2BiNbO_7 and a =

Table 1. Structural parameters of In_2BiNbO_7 prepared by solid state reaction method

Atom	x	y	z	Beq	Occupation factor
In	0.0000	0.0000	0.0000	2.912	1.0
Bi	0.5000	0.5000	0.5000	0.468	0.5
Nb	0.5000	0.5000	0.5000	0.500	0.5
O(1)	-0.1793	0.1250	0.1250	1.000	1.0
O(2)	0.1250	0.1250	0.1250	1.000	1.0

Table 2. Structural parameters of Ga_2BiNbO_7 prepared by solid state reaction method

Atom	x	y	z	Beq	Occupation factor
Ga	0.0000	0.0000	0.0000	2.911	1.0
Bi	0.5000	0.5000	0.5000	0.464	0.5
Nb	0.5000	0.5000	0.5000	0.500	0.5
O(1)	-0.2294	0.1250	0.1250	1.000	1.0
O(2)	0.1250	0.1250	0.1250	1.000	1.0

10.7146(5) Å for In_2BiNbO_7. All the diffraction peaks for M_2BiNbO_7 (M = In and Ga) could be successfully indexed based on the lattice constant and the space group mentioned above. Our X-ray diffraction results shows that Ga_2BiNbO_7 and In_2BiNbO_7 crystallize in the same structure, and 2θ angles of each reflection of In_2BiNbO_7 change with In^{3+} being substituted by Ga^{3+}. The lattice parameter decrease from α = 10.7146(5) Å for In_2BiNbO_7 to α = 10.4685(5) Å for Ga_2BiNbO_7, which indicates a decrease in lattice parameter of the photocatalyst with decrease of the M ionic radii, Ga^{3+} (0.62 Å) < In^{3+} (0.80 Å). The outcome of refinements for In_2BiNbO_7 and Ga_2BiNbO_7 generated the unweighted *R* factors, R_P = 12.93% and 12.47% in space group Fd-3m when the O atoms are included in the model. Bernard *et al.*[15] studied Bi_2CrNbO_7, Bi_2InNbO_7 and Bi_2FeSbO_7 and also observed the large *R* factors (15% to 20%). Zou *et al.*[4] refined the crystal structure of Bi_2InNbO_7 and obtained a large *R* factor (15.5%) for Bi_2InNbO_7, which was ascribed to a slightly modified structure model for Bi_2InNbO_7. Note that the precursors with high purity were used in this study. The influence of minor impurities on the structure of M_2BiNbO_7 (M = In and Ga) can be excluded, which was further supported by the fact that no impurities were detected by EDX analysis. Therefore, we speculate that the slight high R factors for M_2BiNbO_7 (M = In and Ga) are resulted from a slightly modified structure model for M_2BiNbO_7 (M = In and Ga). It should be emphasized that the defects or the disorder/order of a fraction of the atoms can lead to the change of structures, including different bond-distance distributions, thermal displacement parameters and/or occupation factors for some of the atoms.[18]

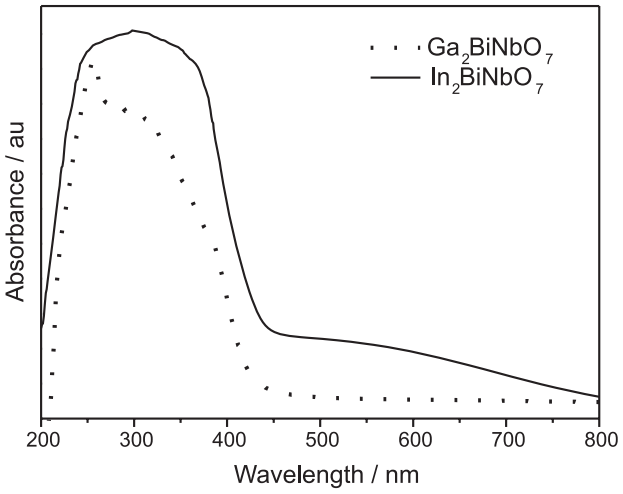

Figure 3. Diffuse reflection spectrum of the cubic M_2BiNbO_7 (M = In and Ga) photocatalysts prepared by a solid state reaction method.

Photophysical properties

Figure 3 shows the results of diffuse reflection spectra of the cubic M_2BiNbO_7 (M = In and Ga) photocatalysts. In contrast to the well-known TiO_2 whose absorption edge is at about 400 nm, the newly synthesized In_2BiNbO_7 and Ga_2BiNbO_7 showed obvious absorption in the visible light region up to 491 and 481 nm (Obtained according to the band gaps of Ga_2BiNbO_7 (E_g = 2.57(8) eV) and In_2BiNbO_7 (E_g = 2.52(5) eV). Then use formula $E_g = hc\lambda^{-1}$) which indicates that M_2BiNbO_7 (M = In and Ga) have the ability to respond to the wavelength of visible light region. Furthermore, the attribution of the second band for In_2BiNbO_7 at about 550 nm is possibly owing to defect energy level within crystal lattice of In_2BiNbO_7 such as oxygen vacancy energy level. It is noteworthy that the band gaps of Ga_2BiNbO_7 and In_2BiNbO_7 are estimated to be 2.57(8) and 2.52(5) eV, indicating narrower band gaps compared to that of Bi_2InTaO_7 (2.92 eV).[19] This may imply that the photoabsorption of M_2BiNbO_7 (M = In and Ga) is stronger than that of Bi_2InTaO_7, which may result in a higher photocatalytic activity of M_2BiNbO_7 (M = In and Ga) than that of Bi_2InTaO_7. In principle, the photoabsorption of the photocatalyst depends on the mobility of electron-hole pairs, which determines the probability of electrons and holes to reach reaction sites on the surface of the photocatalyst.

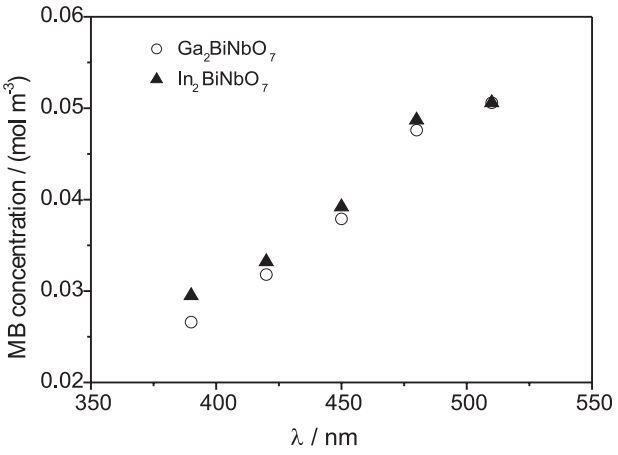

Figure 4. Dependence of methylene blue degradation on the light wavelength (λ) after light irradiation for 90 min over the M_2BiNbO_7 (M = In and Ga) photocatalysts.

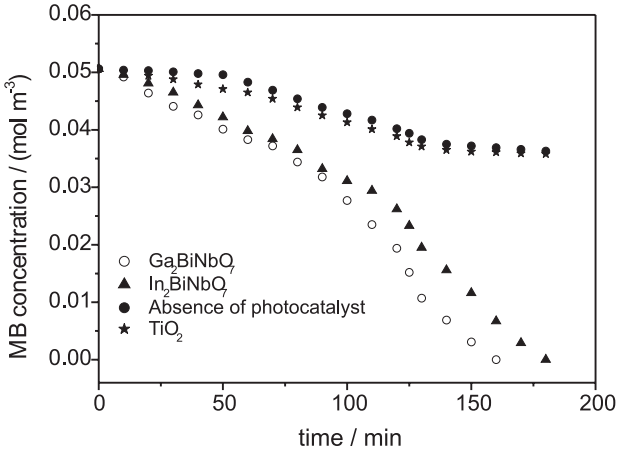

Figure 5. Photocatalytic methylene blue degradation under visible light irradiation (λ > 420 nm) at room temperature in air for 180 min in the presence of M_2BiNbO_7 (M = In and Ga) and TiO_2 (P-25), as well as MB photolysis.

Photocatalytic degradation of methylene blue

In order to know if the photoreaction is induced by light, we studied the effect of the light wavelength on MB degradation. Figure 4 shows dependence of methylene blue degradation on the light wavelength after light irradiation for 90 min over M_2BiNbO_7 (M = In and Ga) using different cut-off filters. The results showed that the photocatalytic activity of M_2BiNbO_7 (M = In and Ga) decreased with increasing light wavelength, indicating that the change of the photocatalytic properties over M_2BiNbO_7 (M = In and Ga) was closely relevant to light wavelength. As a result, the change of the light wavelength will influence directly the amount of photons which participate in the photoreaction. At the same time, photocatalytic degradation of MB could not occur under the dark condition. Thus we may deduce that MB degradation over M_2BiNbO_7 (M = In and Ga) was induced by light. Furthermore, it can be seen from Figure 4 that Ga_2BiNbO_7 showed higher photocatalytic activity (47.4% MB degradation, λ>390 nm; 37.2% MB degradation, λ>420 nm) compared with In_2BiNbO_7 (41.7% MB degradation, λ>390 nm; 34.4% MB degradation, λ>420 nm) not only in UV light region, but also in visible light region.

MB degradation with M_2BiNbO_7 (M = In and Ga) or TiO_2 (P-25) as the photocatalysts under visible light irradiation (λ > 420 nm) are shown in Figure 5. The results showed that the solution color changed from deep blue to colorless and MB concentration in the solution was not detectable after visible light irradiation for 160 min with Ga_2BiNbO_7 as the photocatalyst. The initial rate of MB degradation was about 5.271×10^{-6} mol $s^{-1}m^{-3}$. Simultaneously, a SO_4^{2-} ion concentration of 0.0351 mol m^{-3} was detected in the solution after the photocatalytic reaction for 180 min, indicating that 69.4% of sulphur from MB was turned into sulphate ion. It was obvious that aqueous MB was mainly mineralized rather than bleached under our experimental conditions.

The results also showed that MB concentration in the solution was not detectable after visible light irradiation for 180 min with In_2BiNbO_7 as the photocatalyst. The initial rate of MB degradation was 4.685×10^{-6} mol s^{-1} m^{-3} and a SO_4^{2-} ion concentration of 0.0324 mol m^{-3} was detected in the solution after the photocatalytic reaction, indicating that 64.0% of sulphur from MB was converted into sulphate ion.

In comparison, aqueous MB concentration decreased only from 0.0506 to 0.0358 mol m^{-3} after visible light irradiation for 180 min with TiO_2 as the catalyst, and no SO_4^{2-} ion was detected in the solution after the photoreaction. Photobleaching of MB (MB photolysis) in the absence of catalyst was also carried out under visible light irradiation, as shown in Figure 5. The result indicated that the rate of MB photolysis was almost the same as that of MB degradation with TiO_2 as the catalyst, suggesting that TiO_2 was inactive to MB photocatalytic degradation under visible light irradiation.[12] Liu *et al.*[20] and Xu and Langford[21] studied that alizarin red and X3B dyes could be decomposed over TiO_2 based on visible light driven dye-sensitized phenomena. Tang *et al.*[8] reported that photocatalytic degradation of MB over TiO_2 was also owing to dye-sensitized process under visible light irradiation. Based on above researches, we can draw a conclusion that the effect of dye-sensitized process on photocatalytic degradation of MB over TiO_2 is a little better than the effect of low capacity of visible light irradiation

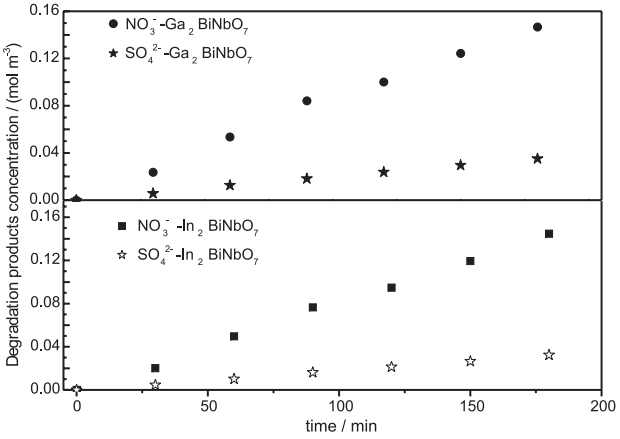

Figure 6. Evolution of SO_4^{2-} and NO_3^- ions in the solution with the M_2BiNbO_7 (M = In and Ga) photocatalysts during the photocatalytic degradation of MB under visible light irradiation ($\lambda > 420$ nm).

to penetrate in a media that contains a fine suspension of TiO_2. Thus the rate of MB photolysis was almost the same as that of MB degradation with TiO_2 as the catalyst.

The ultimate aim of the photodegradation of organic pollutants is to completely convert the toxic organic compounds into inorganics, such as CO_2, SO_4^{2-} or NO_3^-. In the presence of M_2BiNbO_7 (M = In and Ga), the dependence of MB degradation products on the irradiation time is compared in Figure 6. It can be seen that the concentration of SO_4^{2-} or NO_3^- ions increases with the increase of irradiation time. Note that the amount of SO_4^{2-} ions released into the solution is lower than that expected from stoichiometry. The first possible reason is the loss of sulfur-containing volatile compounds such as SO_2. The second probable explanation is given by the partially irreversible adsorption of some SO_4^{2-} ions on the surface of the photocatalyst as already observed.[22] However, the partial irreversible adsorption of SO_4^{2-} ions does not restrain the photocatalytic degradation of pollutants.[22] The higher amount of NO_3^- ions is owing to the stoichiometric ratio *N*/*S* =3 in the initial MB molecule.

In order to monitor whether MB is mineralized or not, the total organic carbon (TOC) was followed during visible light irradiation and the result is shown in Figure 7. The results showed that in the presence of Bi_2InTaO_7 26.7% of TOC decrease was obtained after visible light irradiation for 180 min. On the contrary, in the presence of Ga_2BiNbO_7, a significantly enhanced decrease of the TOC (98.3%) was obtained after 180 min of visible light irradiation. Consequently, the complete mineralization of MB was achieved after 190 min of visible light irradiation in the presence of Ga_2BiNbO_7. Similarly, we also found a decrease of TOC by 96.8% after 180 min of visible light irradiation with In_2BiNbO_7 as the photocatalyst.

Photocatalytic water splitting

Figure 8 shows the photocatalytic H_2 evolution from pure water under UV light irradiation over the M_2BiNbO_7 (M = In and Ga) photocatalysts. H_2 evolution rates and some physical properties are listed in Table 3. It can be seen from Figure 8 that the activities of M_2BiNbO_7 (M = In and Ga) are different and the results are listed in Table 3. It was found that H_2 evolution rates are estimated to be 72.6 μmol h^{-1} for Ga_2BiNbO_7 and 54.3 μmol h^{-1} for In_2BiNbO_7, indicating that Ga_2BiNbO_7 exhibits a larger activity than In_2BiNbO_7. The influence of the UV light irradiation was also investigated by light on/off shutter studies over M_2BiNbO_7 (M = In and Ga). The H_2 evolution stopped by terminating the UV light irradiation, indicating that the reactions of H_2 evolution were initiated by UV light

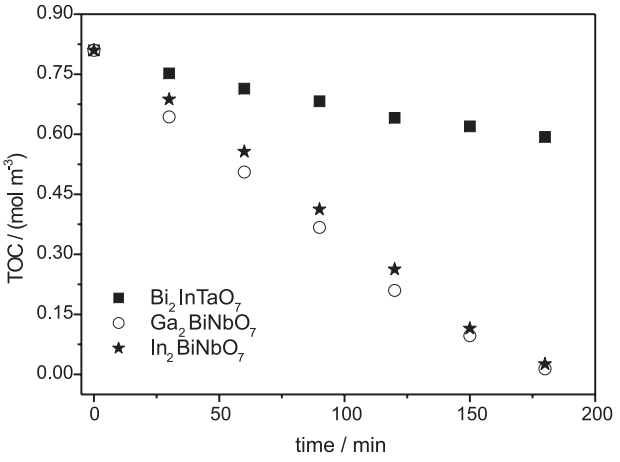

Figure 7. Disappearance of total organic carbon (TOC) during the photocatalytic degradation of MB by photocatalysis (with Bi_2InTaO_7 or M_2BiNbO_7 (M = In and Ga)) under visible light irradiation ($\lambda > 420$ nm).

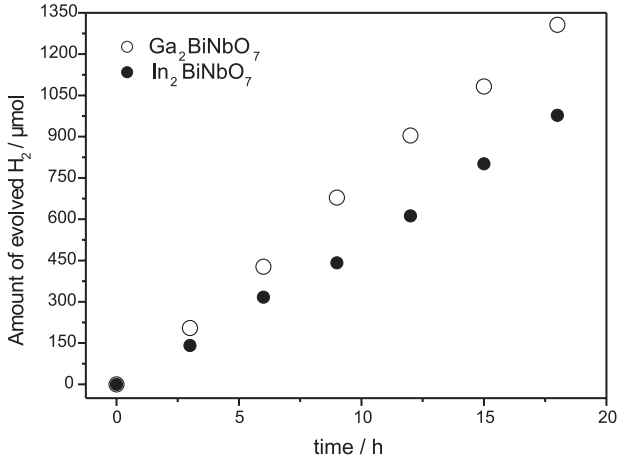

Figure 8. Photocatalytic H_2 evolution over M_2BiNbO_7 (M = In and Ga) from pure water under ultraviolet light irradiation. (Wavelength: λ = 390 nm, Catalyst: 1 g, H_2O: 300 mL, Light source: 400 W high-pressure Hg lamp.)

Table 3. Physical properties and formation rates of H_2 or O_2 evolutions from pure water over M_2BiNbO_7(M=In and Ga)

Catalyst	Lattice[a]	Lattice[b]	M-O1-M	Band gap /	Surface area /	Rate of gas / (μmol h^{-1})	
	Parameter / (Å)	distortion	angle[c] / (°)	(eV)	(m^2 g^{-1})	H_2[d]	O_2[d]
In_2BiNbO_7	10.7146(5)	0.054(3)	136.40(3)	2.52(5)	1.45	54.3	26.6
Ga_2BiNbO_7	10.4685(5)	0.104(4)	166.72(4)	2.57(8)	1.36	72.6	35.7

[a] The lattice parameter was obtained by the Rietveld structure refinement; [b] Lattice distortion was defined as 0.375—the O(48f) parameter x; [c] Angle between the corner-linked MO_6 (M=Bi and Nb) polyhedral; [d] Measured by a 400 W Hg lamp (catalyst: 1.0 g; pure water: 300 cm^3; non co-catalyst was loaded onto the catalyst surface).

irradiation. In the second run, almost the same H_2 evolution rate was obtained after the system was evacuated. In order to compare the catalytic activities of M_2BiNbO_7 (M = In and Ga) with that of TiO_2, water splitting with P25 as the catalyst was conducted. In the presence of P25, the rate of H_2 evolution from pure water was about 1.4 μmol h^{-1} in the first 15 h, which shows much lower activity than that of M_2BiNbO_7 (M = In and Ga).

Based on the observed H_2 and O_2 evolution from pure water, it can be concluded that the conduction band levels of M_2BiNbO_7 (M = In and Ga) are more negative than that of H_2 evolution and the valence band levels are more positive than that of O_2 evolution. Namely, M_2BiNbO_7 (M = In and Ga) have proper band structures for the reduction of H^+ to H_2 and oxidation of H_2O to O_2, respectively. Figure 9 shows suggested band structures of M_2BiNbO_7 (M = In and Ga). Recently, the electronic structures of $InMO_4$ (M = V, Nb and Ta) and $BiVO_4$ were reported by Oshikiri et al. based on the first principles calculations.[23] The conduction bands of the $InMO_4$ (M = V, Nb and Ta) photocatalysts are composed of a small indium 5s orbital component (about 20%) and a dominant d orbital component coming from vanadium 3d, niobium 4d and tantalum 5d orbitals, respectively. The valence bands of the $BiVO_4$ photocatalyst are composed of a small Bi 6s orbital component and a dominant O 2p orbital component. The band structures and valence band levels of M_2BiNbO_7 (M = In and Ga) should be similar to $InMO_4$ (M = V, Nb and Ta) and $BiVO_4$ due to their similar distorted pyrochlore-type structure. Therefore, we conclude that the conduction band of In_2BiNbO_7 is consisted of Nb 4d and In 5s. The valence band of In_2BiNbO_7 is consisted of a small Bi 6s orbital component and a dominant O 2p orbital component. Similarly, the conduction band of Ga_2BiNbO_7 is consisted of Nb 4d and Ga 4s. The valence band of Ga_2BiNbO_7 is almost the same as that of In_2BiNbO_7.

These photocatalysts consist of a three-dimensional network structure of corner-linked MO_6 (M = Bi, Nb) octahedra and the MO_6 octahedra are connected into chains with In^{3+} ions or Ga^{3+} ions. The shapes of AO_8 and BO_6 polyhedra vary with the O(48f) parameter x in the pyrochlore-type $A_2B_2O_7$ structure. The O(48f) parameter x is 0.375 when the O(48f) atoms are located at the position of the related fluorite-type structure.[24] Thus, information on the lattice distortion can be obtained from the O(48f) parameter x in the pyrochlore-type $A_2B_2O_7$ structure. The lattice distortion is defined according to the distortion of BO_6 polyhedral from the regular octahedral. The O(48f) parameter x of these photocatalysts were attained from the Rietveld structure refinement and the results are described in Table 3. The lattice distortion was estimated to be 0.104(4) for Ga_2BiNbO_7 and 0.054(3) for In_2BiNbO_7 because the lattice distortion is equal to 0.375—the O(48f) parameter x. During the process of photocatalytic water splitting into H_2 and O_2, charge separation is necessary to inhibit the recombination of the photoinduced electrons and holes. The lattice distortion is one important parameter for charge separation, and will result in the enhanced photocatalytic activity.[25,26] In other words, for the photocatalysts with same crystal and electronic structure, the higher photocatalytic activity is mainly resulted from the larger lattice distortion. This conclusion is confirmed by the fact that Ga_2BiNbO_7 with larger lattice distortion (0.104(4)) shows higher photocatalytic activity compared to In_2BiNbO_7 with the lattice distortion of 0.054(3).

The research on the luminescent properties has given a conclusion that the closer the angle between the corner-linked octahedral is to 180°, the more the excited

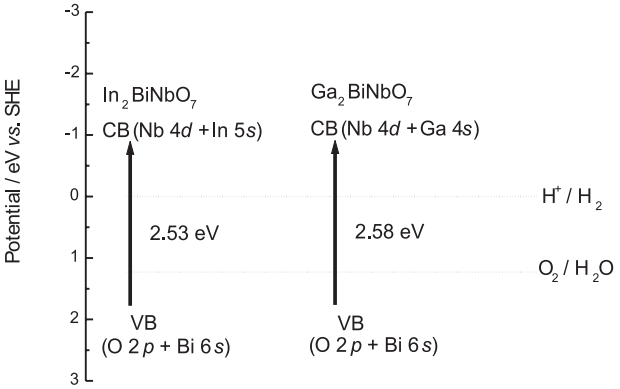

Figure 9. Suggested band structures of the M_2BiNbO_7 (M = In and Ga) photocatalysts.

state is delocalized.[27] This indicates that the photoinduced electrons and holes can move easily if the angle between the corner-linked octahedral is close to 180°. The mobility of the photoinduced electrons and holes also influences the photocatalytic activity because it influences the probability of electrons and holes to reach reaction sites on the catalyst surface. The angles between the corner-linked MO_6 (M = Bi and Nb) octahedral, *i.e.* the M–O1–M bond angles were attained by the Rietveld structure refinement and the results are shown in Table 3. Comparing the M–O1–M bond angles and the photocatalytic activities of Ga_2BiNbO_7 with those of In_2BiNbO_7, we can find that the closer the M–O1–M bond angle is to 180°, the higher the photocatalytic activity is. The crystal structures of these photocatalysts are almost the same, but their electronic structures are considered to be different. For the M_2BiNbO_7 (M = In and Ga) photocatalysts, indium and gallium are p-block metal elements, indicating that the photocatalytic activity may be affected by not only the crystal structure but also the electronic structure of the photocatalysts. Both of the lattice distortion and the angles between the corner-linked MO_6 (M = Bi and Nb) octahedral are possible to influence the photocatalytic activities of M_2BiNbO_7 (M = In and Ga). Although direct absorption of photons by the semiconductor oxide can produce electron–hole pairs in the catalysts, the gases evolution (H_2 or O_2) can not be observed from pure water under visible light irradiation in our experiments, possibly indicating that the larger energy than the band gap is necessary for splitting water into H_2 and O_2 by photocatalysis.

Conclusions

We prepared single phase of the M_2BiNbO_7 (M = In and Ga) photocatalysts by solid state reaction method and investigated the structural, optical absorption and photocatalytic properties. XRD results indicated that these compounds crystallize in the pyrochlore-type structure, cubic system with space group Fd-3m. The lattice parameters of Ga_2BiNbO_7 and In_2BiNbO_7 are 10.4685(5) and 10.7146(5) Angstrom respectively. The band gaps of Ga_2BiNbO_7 and In_2BiNbO_7 were estimated to be about 2.57(8) and 2.52(5) eV and the compounds show strong optical absorption in the visible region ($\lambda >$ 420 nm). In addition, H_2 or O_2 evolution was observed from pure water respectively with M_2BiNbO_7 (M = In and Ga) as the photocatalysts under ultraviolet light irradiation. In the presence of M_2BiNbO_7 (M = In and Ga), photocatalytic decomposition of aqueous MB could be achieved under visible light irradiation. At the same time, the mineralization of aqueous MB led to the generation of SO_4^{2-} and NO_3^- and to the marked decrease of TOC during the reaction, which suggests that M_2BiNbO_7 (M = In and Ga)/VIS system may be regarded as an effective method for treatment of the wastewater from the textile industry.

Acknowledgments

This work was supported by a grant from the Natural Science Foundation of Jiangsu Province (No. BK2006130).

Supplementary Information

Structural formula of methylene blue, the schematic structural diagram of the cubic M_2BiNbO_7 (M = In and Ga) photocatalysts, plot of $(\alpha h\nu)^2$ *versus* $h\nu$ for the M_2BiNbO_7 (M = In and Ga) photocatalysts, effect of photocatalyst concentration on photocatalytic methylene blue degradation under visible light irradiation ($\lambda >$ 420 nm) for 90 min, photocatalytic methylene blue degradation under visible light irradiation ($\lambda >$ 420 nm) at room temperature in the presence of Bi_2MNbO_7 (M = In, Al and Ga) and Bi_2InTaO_7, photocatalytic O_2 evolution over M_2BiNbO_7 (M = In and Ga) from pure water under ultraviolet light irradiation, physical properties of Bi_2MNbO_7 (M = In, Al and Ga) and Bi_2InTaO_7 are available free of charge at http://jbcs.sbq.org.br, as PDF file.

References

1. Honda, K.; Fujishima, A.; *Nature* **1972**, *238*, 37.
2. Zou, Z.; Ye, J.; Sayama, K.; Arakawa, H.; *Nature* **2001**, *414*, 625.
3. Zou, Z.; Ye, J.; Arakawa, H.; *J. Phys. Chem. B* **2002**, *106*, 13098.
4. Zou, Z.; Ye, J.; Arakawa, H.; *J. Mater. Sci. Lett.* **2000**, *19*, 1909.
5. Zou, Z.; Ye, J.; Arakawa, H.; *Chem. Mater.* **2001**, *13*, 1765.
6. Zou, Z.; Ye, J.; Arakawa, H.; *J. Phys. Chem. B* **2002**, *106*, 517.
7. Zou, Z.; Ye, J.; Oka, K.; Nishihara, Y.; *Phys. Rev. Lett.* **1998**, *80*, 1074.
8. Tang, J.; Zou, Z.; Yin, J.; Ye, J.; *Chem. Phys. Lett.* **2003**, *382*, 175.
9. Matos, J.; Laine, J.; Herrmann, J. M.; *J. Catal.* **2001**, *200*, 10.
10. Qu, P.; Zhao, J.; Shen, T.; Hidaka, H.; *J. Mol. Catal. A* **1998,** *129*, 257.
11. Xu, Y. M.; Langford, C. H.; *Langmuir* **2001**, *17*, 897.
12. Asahi, R.; Morikawa, T.; Ohwaki, T.; Aoki, K.; Taga, Y.; *Science* **2001**, *293*, 269.
13. Li, F. B.; Li, X. Z.; *Appl. Catal. A* **2002**, *228*, 15.
14. Li, F. B.; Li, X. Z.; *Chemosphere* **2002**, *48*, 1103.

15. Bernard, D.; Pannetier, J. ; Lucas, J.; *Ferroelectrics* **1978**, *21*, 429.
16. Golovshchikove, G. I.; Isupov, V. A. ; Tutov, A. G.; Nikove, A. G.; Myl, I. E.; Nikitina, P. A.; Tulinova, O. I.; *Sov.Phys.Solid State* **1973**, *14*, 2539.
17. Izumi, F.; *J. Crystallogr. Assoc. Jpn.* **1985**, *27*, 23.
18. Xu, J.; Emge, T.; Ramanujachary, K. V.; Hohn, P.; Greenblatt, M.; *J. Solid State Chem.* **1996**, *125*, 192.
19. Wang, J. H.; Zou, Z.; Ye, J.; *Mater. Sci. Forum* **2003**, *423*, 485.
20. Liu, G.; Wu, T.; Zhao, J.; Hidaka, H.; Serpone, N.; *Environ. Sci. Technol.* **1999**, *33*, 2081.
21. Xu, Y. M.; Langford, C. H.; *Langmuir* **2001**, *17*, 897.
22. Lachheb, H.; Puzenat, E.; Houas, A.; Ksibi, M.; Elaloui, E.; Guilard, C.; Herrmann, J. M.; *Appl. Catal. B* **2002**, *39*, 75.
23. Oshikiri, M.; Boero, M.; Ye, J.; Zou, Z.; Kido, G.; *J. Chem. Phys.* **2002**, *117*, 7313.
24. Subramanian, M. A.; Aravamudan, G.; Subba, G. V.; *Prog. Solid State Chem.* **1983**, *15*, 55.
25. Inoue, Y.; Kohno, M.; Ogura, S.; Sato, K.; *Chem. Phys. Lett.* **1997**, *267*, 72.
26. Kudo, A.; Kato, H.; Nakagawa, S.; *J. Phys. Chem. B* **2000**, *104*, 571.
27. Wiegel, M.; Middel, W.; Blasse, G.; *J. Mater. Chem.* **1995**, *5*, 981.

Received: December 7, 2005
Published on the web: September 26, 2006

J. Braz. Chem. Soc., Vol. 17, No. 7, S1-S3, 2006.
Printed in Brazil - ©2006 Sociedade Brasileira de Química
0103 - 5053 $6.00+0.00

Photophysical and Photocatalytic Properties of Novel M_2BiNbO_7 (M = In and Ga)

Jingfei Luan,[*,a] Shourong Zheng,[a] Xiping Hao,[b] Guoyou Luan,[c] Xiaoshan Wu[b] and Zhigang Zou[d]*

[a]*State Key Laboratory of Pollution Control and Resource Reuse, School of Environment, Nanjing University, Nanjing, 210093 People's Republic of China*

[b]*National Laboratory of Solid State Microstructures, Nanjing University, Nanjing 210093, People's Republic of China*

[c]*State Key Laboratory of Catalysis, Dalian Institute of Chemical Physics, Chinese Academy of Sciences, Dalian 116023, People's Republic of China*

[d]*Eco-Materials and Renewable Energy Research Center, Nanjing University, Nanjing 210093, People's Republic of China*

The structural formula of MB was shown in Figure S1. The structure of M_2BiNbO_7 (M = In and Ga) is shown in Figure S2. The structure of M_2BiNbO_7 (M = In and Ga) is composed of the three-dimensional network of MO_6 (M = Bi, Nb), stacked along [110] and separated by a unit cell translation (10.7146(5) or 10.4685(5) Å).

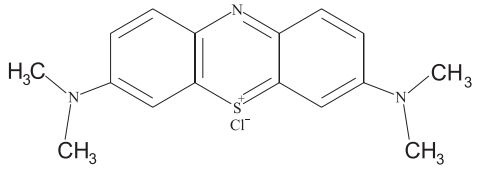

Figure S1. Structural formula of methylene blue.

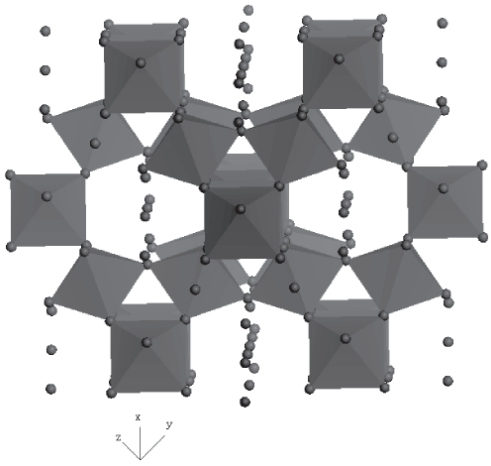

Figure S2. The schematic structural diagram of the cubic M_2BiNbO_7 (M = In and Ga) photocatalysts. Three-dimensional network of MO_6 stacked along [110] and separated by a unit cell translation.

For a crystalline semiconductor, it is commonly accepted that the optical absorption near the band edge follows the equation:[1,2] $\alpha h\nu = A(h\nu - E_g)^n$. A, α, E_g and ν are proportional constant, absorption coefficient, band gap, and light frequency, respectively. Within this equation, n determines the character of the transition in a semiconductor. E_g and n can be calculated by the following steps: plot $\ln(\alpha h\nu)$ versus $\ln(h\nu - E_g)$ with an approximative value of E_g, then decide the value of n with the slope of the straightest line near the band edge, at last, plot $(\alpha h\nu)^{1/n}$ versus $h\nu$ and evaluate the band gap E_g by extrapolating the straightest line to the $h\nu$ axis intercept. Based on above method, the value of n for M_2BiNbO_7 (M = In and Ga) was calculated to be 0.5 from Figure 3 of the paper, indicating that the optical transitions for these oxides are directly allowed. Figure S3 shows the Plot of $(\alpha h\nu)^2$ versus $h\nu$ for Ga_2BiNbO_7 and In_2BiNbO_7. Figure S2 showed that M_2BiNbO_7 (M = In and Ga) consisted of the network of MO_6, which is built by forming infinite corner-sharing MO_6 octahedra with the zigzag chains along [110]. This suggests that photogenerated electron-hole pairs in the M_2BiNbO_7 (M = In and Ga) photocatalysts can move easily in this direction, which may result in a high photocatalytic activities of M_2BiNbO_7 (M = In and Ga).

Figure S4 shows the effect of photocatalyst concentration on photocatalytic methylene blue degradation under visible light irradiation at room temperature in air for 90 min. It could be seen that MB concentration decreased with increasing photocatalyst concentration when the photocatalyst concentration was

*e-mail: jfluan@nju.edu.cn

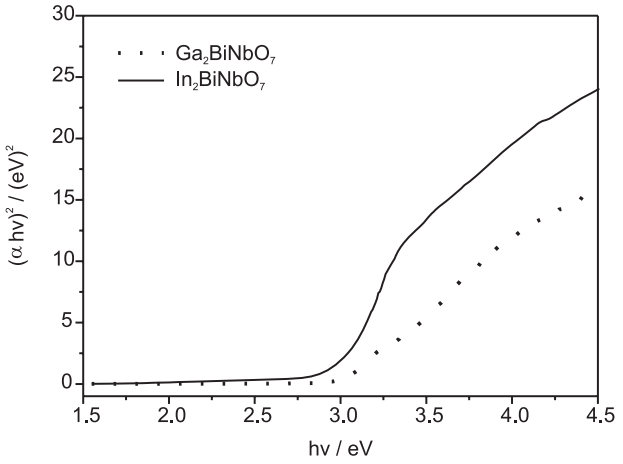

Figure S3. Plot of $(\alpha h\nu)^2$ *versus* hν for the M_2BiNbO_7 (M = In and Ga) photocatalysts.

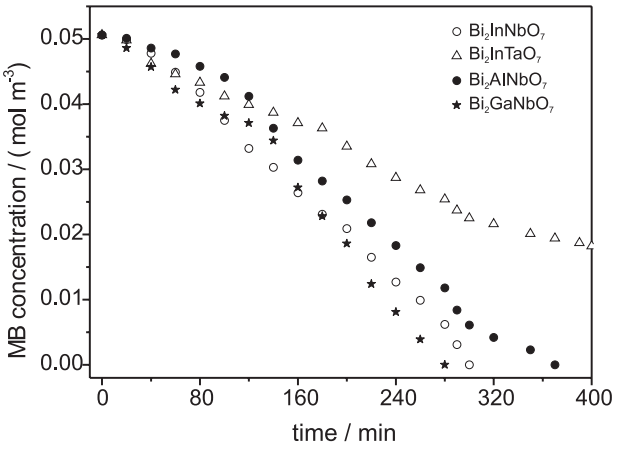

Figure S5. Photocatalytic methylene blue degradation under visible light irradiation (λ > 420 nm) at room temperature in the presence of Bi_2MNbO_7 (M = In, Al and Ga) and Bi_2InTaO_7.

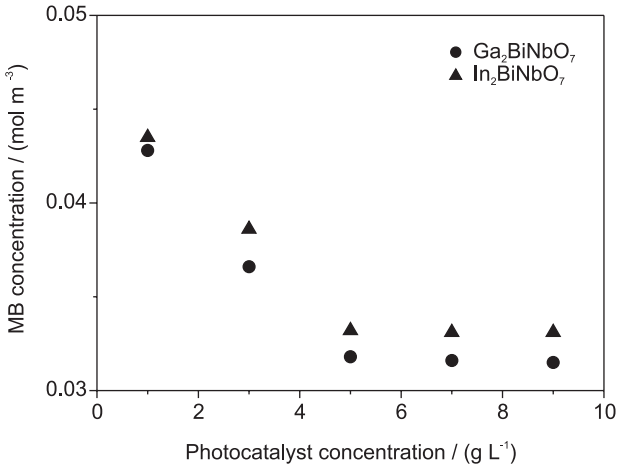

Figure S4. Effect of photocatalyst concentration on photocatalytic methylene blue degradation under visible light irradiation (λ > 420 nm) at room temperature in air for 90 min.

lower than 5 g L^{-1}. While MB concentration kept unchanging with increasing photocatalyst concentration when the photocatalyst concentration was higher than 5 g L^{-1}. The possible reason is the low capacity of visible light irradiation to penetrate in a media that contains a fine suspension of large amount of photocatalyst. Thus we chose 5 g L^{-1} as photocatalyst concentration.

Figure S5 shows photocatalytic methylene blue degradation under visible light irradiation (λ > 420 nm) in the presence of Bi_2MNbO_7 (M = In, Al and Ga) and Bi_2InTaO_7. The results showed that the solution color changed from deep blue to colorless and MB concentration in the solution was not detectable after visible light irradiation for 280, 300 and 370 min with Bi_2GaNbO_7, Bi_2InNbO_7 and Bi_2AlNbO_7 as the photocatalysts, respectively. However, MB concentration decreased only from 0.0506 to 0.0182 mol m^{-3} after visible light irradiation for 400 min with Bi_2InTaO_7 as the catalyst. The initial rates of MB degradation for Bi_2GaNbO_7, Bi_2InNbO_7, Bi_2AlNbO_7 and Bi_2InTaO_7 were about 3.012×10^{-6}, 2.811×10^{-6}, 2.279×10^{-6} and 1.350×10^{-6} mol s^{-1} m^{-3}, respectively. Table S1 shows the physical properties of Bi_2MNbO_7 (M = In, Al and Ga) and Bi_2InTaO_7. Table 3 of the paper shows the physical properties of M_2BiNbO_7(M=In and Ga). It could be seen that the surface areas of these compounds were nearly the same and their particle size were also very similar. Thus we can draw a conclusion that the photocatalytic activity of these compounds is as following order: $Ga_2BiNbO_7 > In_2BiNbO_7 > Bi_2GaNbO_7 > Bi_2InNbO_7 > Bi_2AlNbO_7 > Bi_2InTaO_7$.

Table S1. Physical properties of Bi_2MNbO_7 (M = In, Al and Ga) and Bi_2InTaO_7

Catalyst	Lattice[a] Parameter / (Å)	Average particle size / (μm)	Band gap / (eV)	Surface area / (m^2 g^{-1})	crystal structure
Bi_2InNbO_7	10.7793(2)[3]	1.4	2.7[3]	1.53	Pyrochlore type, cubic system with space group Fd-3m
Bi_2GaNbO_7	10.7342(2)[4]	1.5	2.75[4]	1.51	
Bi_2AlNbO_7	10.7171(2)[4]	1.4	2.9[4]	1.54	
Bi_2InTaO_7	10.7612(2)[5]	1.3	2.92[5]	1.57	

[a] The lattice parameter was obtained by the Rietveld structure refinement; [b] Measured by a 300 W Xe arc lamp (a cut-off filter λ > 420 nm; catalyst: 0.5 g; 100 mL methylene blue solution).

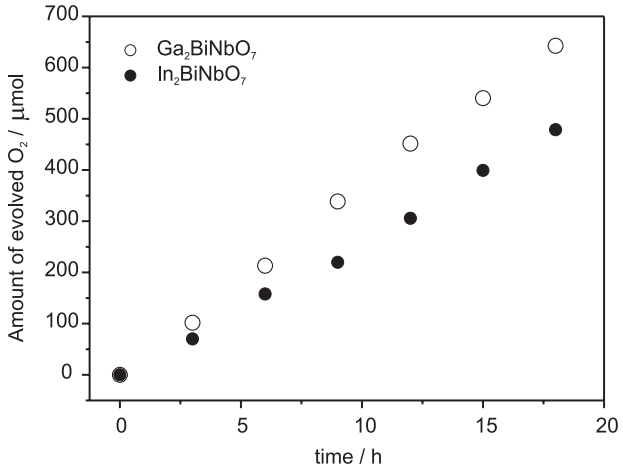

Figure S6. Photocatalytic O_2 evolution over M_2BiNbO_7 (M = In and Ga) from pure water under ultraviolet light irradiation. (Wavelength: $\lambda = 390$ nm, Catalyst: 1 g, H_2O: 300 mL, Light source: 400 W high-pressure Hg lamp.)

Figure S6 shows the photocatalytic O_2 evolution from pure water under UV light irradiation over the M_2BiNbO_7 (M = In and Ga) photocatalysts and the results are described in Table 3 of the paper. Similar to H_2 evolutions, the O_2 evolutions increased with illumination time and O_2 evolution rates also varied according to the following order: $Ga_2BiNbO_7 > In_2BiNbO_7$.

References

1. Butler, M. A.; *J. Appl. Phys.* **1977**, *48*, 1914.
2. Tauc, J.; Grigorovici, R.; Vancu, A.; *Phys. Stat. Sol.* **1966**, *15*, 627.
3. Zou, Z.; Ye, J.; Arakawa, H.; *J. Mater. Sci. Lett.* **2000**, *19*, 1909.
4. Zou, Z.; Ye, J.; Arakawa, H.; *Chem. Mater.* **2001**, *13*, 1765.
5. Wang, J. H.; Zou, Z.; Ye, J.; *Mater. Sci. Forum* **2003**, *423*, 485.